Vegetation restoration changes topsoil biophysical regulations of carbon fluxes in an eroding soil landscape

Jianye Li[1,2], Bojie Fu[1,2]*, Shuguang Liu[3,4], Paul Dargush[5], Guangyao Gao[1,2], Jianbo Liu[6], Fangli Wei[1,2]

[1]State Key Laboratory of Urban and Regional Ecology, Research Center for Eco-Environmental Sciences, Chinese Academy of Sciences, Beijing, 100085, P.R. China

[2] University of Chinese Academy of Sciences, Beijing, 100049, P.R. China

[3] National Engineering Laboratory of Applied Technology of Forestry & Ecology for Southern China, Central South University of Forestry and Technology, Changsha, 410004, P.R. China

[4] Faculty of Life Science and Technology, Central South University of Forestry and Technology, Changsha, 410004, P.R. China

[5] School of Earth and Environmental Sciences, University of Queensland, Campbell Rd, Saint Lucia, QLD 4072, Australia

[6] Tianjin Key Laboratory of Water Resources and Environment, Tianjin Normal University, Tianjin, 300387, P.R. China

This article has been accepted for publication and undergone full peer review but has not been through the copyediting, typesetting, pagination and proofreading process which may lead to differences between this version and the Version of Record. Please cite this article as doi: 10.1002/ldr.3175

*Corresponding author

Prof. Dr. Bojie Fu

State Key Laboratory of Urban and Regional Ecology

Research Center for Eco-Environmental Sciences

Chinese Academy of Sciences

P. O. Box 2871, Beijing 100085, China

E-mail: bfu@rcees.ac.cn

Tel: +86-10-62923557

Fax: +86-10-62923557

Abstract: The dynamics of biophysical regulations of carbon fluxes can have a major effect on an ecosystems carbon budget. Only a handful of comprehensive assessments of such dynamics exist. To better understand the carbon cycle we measured all major carbon flux by biophysical regulations including rainfall, runoff, infiltration and sediment yield at eight runoff plots in an eroding soil landscape on the Chinese Loess Plateau; a typical vegetation restoration area for the region. Results show that topsoil carbon flux by infiltration into deep soil layers was the largest efflux from topsoil in plots with vegetation, followed by runoff and sediment carbon effluxes. On the contrary, the carbon flux by sediment was the largest efflux from topsoil in plot without vegetation, followed by infiltration and runoff carbon effluxes. Total topsoil carbon flux by biophysical regulations to the deep layer is about 71 ±10 % of the typical carbon sequestration rate in the region. Topsoil carbon sequestration capacity might be underestimated by up to 43 ±3 % if the infiltrated carbon was not factored into estimates. The results of this study improve understanding of soil carbon dynamics and expand the dynamic carbon replacement hypothesis; photosynthesis replaces not only lateral carbon lost by erosion but also vertical carbon lost by infiltration.

Keywords: carbon flux by biophysical regulation, dynamic carbon replacement, carbon sequestration, vegetation restoration, water-driven erosion

1. Introduction

Soil carbon (SC) plays an important role in the global carbon cycle; most of the world's carbon is stored in the soil (Chappell et al., 2015; Lal, 2003). Carbon movement induced by rainfall storms can have an extensive effect on the carbon budget of terrestrial ecosystems (Lal, 2003; Lal & Pimentel, 2008; Liu et al., 2003; Young et al., 2014; Yue et al., 2016). Soil erosion destroys the physical protection of carbon in soil aggregates and accelerates decomposition, which impacts SC stocks and alters CO_2 fluxes exchanged with the atmosphere through mineralization of soil organic matter to CO_2 (Zhang et al., 2015). Soil seals caused by the breakage of aggregates during erosion also affect infiltration process and the associated vertical carbon flux by infiltration (Li et al., 2015; Rieckh et al., 2014). These carbon fluxes by biophysical regulations, which can be bound with moving sediments (sediment-bound carbon (SBC)) or in the form of dissolved carbon (DC) (Nie et al., 2014), are mainly driven by corresponding hydrological fluxes during rainfall storms (Li et al., 2016).

Carbon fluxes are influenced by numerous factors, such as surface runoff, sediment transport, infiltration leaching (Boix-Fayos et al., 2015; Ma et al., 2014; Schreiber, 1999), topography and physical and chemical properties of soil (Clark et al., 2004; Zhang et al., 2013), ratios of C:N in soil (Aitkenhead-Peterson et al., 2007; Alvarez-Cobelas et al., 2012),

rainstorm characteristics (e.g., rainfall intensity, rainfall amount and storm duration) (Nie et al., 2016; Polyakov & Lal, 2004), vegetation cover and land use changes (Bouchoms et al., 2017; Hu et al., 2018; Jacinthe et al., 2004). In an eroding soil landscape, most of the SC is lost through physical removal by water during rainfall storms (Nie et al., 2014). Leaching of DC by infiltration to subsoil layers resulting from water-driven erosion also leads to vertical carbon loss from topsoil (Ma et al., 2014). The soil aggregate is an important factor affecting SC stocks, which is sensitive to land use management and soil erosion (Razafimbelo et al., 2008). Vegetation restoration increases soil aggregate stability and cohesion, changes physical and chemical properties of soil, reduces sediment and surface runoff and increases infiltration into subsoil layers (Elena et al., 2017; Pohl et al., 2012). In addition, SC loss increases with rainfall intensity (Alvarez-Cobelas et al., 2012).

Knowledge of the distribution, quantity, and dynamics of biophysical regulations of carbon fluxes during rainfall storms is important for both improving model-based projections of the carbon cycle and understanding the role of carbon fluxes by biophysical regulations in SC pools dynamics. Lateral and vertical carbon fluxes have been studied extensively (Doetterl et al., 2016; Rieckh et al., 2014; Yue et al., 2016). But few previous studies have examined both lateral and vertical carbon flux. Different sizes of runoff plots have been used to observe lateral carbon fluxes (Martinez-Mena et al., 2008; Schiettecatte et al., 2008a; Schiettecatte et al., 2008b) and vertical carbon fluxes released to the atmosphere during soil erosion process (Bremenfeld et al., 2013; Hemelryck et al., 2010; Wang et al., 2014). A number of studies have quantified the amount of SC exported during rainfall storms

(Müller-Nedebock & Chaplot, 2015; Quinton et al., 2006; Wang et al., 2017). A few studies have also reported on the links between soil erosion and DC fluxes (Kindler et al., 2011). In addition, the role of vertical DC flux has been reported as a carbon output for topsoil layers and a carbon input for deeper soil layers (Ma et al., 2014; Rumpel & Kogel-Knabner, 2011). However, most data on vertical DC fluxes were collected in places with limited erosion (Brye et al., 2001; Rieckh et al., 2014). The literature is still unclear on how to distinguish between lateral (DC flux in surface runoff) and vertical (DC flux in infiltration) DC flux (Doetterl et al., 2016). Vertical DC flux has not been observed or included when calculating the carbon sequestration capacity in most previous studies (Deng et al., 2017; Deng et al., 2014b; Lal, 2004).

The topsoil layer is easily affected by environmental factors and water-driven erosion (Gauder et al., 2016), with topsoil carbon fluxes by biophysical regulations being mainly induced by rainfall storms. Few studies have accounted for the quantity of all the major topsoil carbon fluxes by biophysical regulations induced by rainfall storms in eroding soil landscapes. The purpose of to the research presented in this paper is to develop a better understanding of the impacts of different vegetation restoration conditions on topsoil carbon fluxes by biophysical regulations and to investigate the quantitative relationships between carbon fluxes and influencing factors. Our research questions are: (1) explore the quantitative relationship of the topsoil carbon fluxes and biophysical regulations in an eroding soil landscape; and (2) understanding the role of topsoil carbon fluxes by biophysical regulations in SC pools dynamics.

2. Material and methods

2.1. Study area

Data was collected from the Yangjuangou catchment, which is located in Yan'an city of Shaanxi province, China. The longitude is 36° 42′ N and latitude is 109° 31′ E. The area of the catchment is 2.02 km^2. Slope gradients in the catchment range from 10° to 30° and its elevation ranges from 1050 to 1298 m a.s.l.. Soil properties are listed in Table S1. The soil is derived mainly from loess, which has a deep depth about 50 - 200 m. The soil type is Calcaric Cambisol with a uniform texture and weak structure (Li et al., 2003). The gully density of the catchment is 2.74 km km^{-2}. This hill-and-gully landscape is typical on the Loess Plateau. In the past the area was heavily eroded but now it is a typical vegetation restoration area, with restoration carried out under the Grain for-Green Project in 1999 (Fu et al., 2017).

The growing season for most of the deciduous plants in the region is from May to September. The mean annual air temperature is 9.8±0.8 °C. The mean annual precipitation is 531.0 mm and the average precipitation during the growing season is 422 mm (Jiao et al., 2016). The main land use types are forest, grassland and shrubland.

2.2. Measurement of soil erosion and carbon flux

Eight runoff plots were setup on the hill-slopes that had vegetation cover (Figure 1) of" *Robinia pseudoacacia* (A1, 2×10 m); *Prunus armeniaca L* (A2, 2×10 m); *Spiraea salicifolia* (S1, 2×10 m); *Hippophae rhamnoides* (S2, 2×10 m); a *Stipa bungeana* community (H1, 3×10 m); a mixed herbaceous (*Stipa bungeana*, *Liquorice*, *Lespedeza* , *Salsola collina et.al.*)

community (H2, 3×10 m); an *Artemisia scoparia* community (H3, 3×10 m); and a bare soil (CK, 3×10 m). The vegetation community characteristics in each plot are listed in Table S1. All the plots had similar slope gradients of about 20^{o}. Each runoff plot was surrounded by polyvinyl chloride (PVC) boards. The boards embedded into the soil (500 mm deep) were used to separate the sediment yield and surface runoff in and out of the plots. At the bottom edge of each runoff plot, a U shape PVC runoff gathering pit was installed to transfer the surface runoff to a collecting tank.

In total, nine rainfall events were recorded at our field sites between July and October 2016. The rainfall events were numbered from 1 to 9 according to the corresponding sampling dates from start (July 15^{th}) to end (October 8^{th}). The rainfall characteristics of each event are listed in Table S1. After each rainfall event, the sediments both in runoff gathering pit and collecting tank were collected, dried, and weighed to measure carbon concentration in the sediment (TC_{CS}), including organic carbon concentration (OC_{CS}) and inorganic carbon concentration (IC_{CS}). These sediment weights were also used to compute the sediment concentration in runoff (S_C), a key variable in estimating the total soil loss (S) per plot. S was calculated as a product of runoff volume (R) and S_C. The R from each plot was measured after each rainfall event. Runoff into the collecting tanks was collected in 250 mL plastic bottles (then stored at 4℃ in a refrigerator) for monitoring the carbon concentration in runoff (TC_{CR}), which including dissolved organic carbon concentration (OC_{CR}) and dissolved inorganic carbon concentration (IC_{CR}).

After each rainfall event, a soil water sampler was installed and used for collecting soil

infiltration water (I). The Model 1900 Soil Water Sampler (Doetterl et al., 2016; Zhao et al., 2013) used in the experiment comes fully assembled. This instrument is a large-volume sampler designed for near-surface installation at 50 mm depth in the study. Two sets of soil water samplers were installed in each plot, one was 2.5 meters from the top edge of the plot and one was 7.5 meters from the top edge. The infiltration water samples collected were put in plastic bottles (250 mL) and kept in a refrigerator (4℃) for later measuring dissolved carbon concentration in infiltration (TC_{CI}), including dissolved organic carbon concentration (OC_{CI}) and dissolved inorganic carbon concentration (IC_{CI}).

One set of simple rain gauge was installed in each of the plots with no rainfall interception (H1, H2, H3, and CK). Under the woody vegetation cover, six sets of simple rain gauges were installed in each of the plots (A1, A2, S1, S2) for collecting throughfall. After each rainfall event, rainfall or throughfall volume (P) was measured and collected in a plastic bottle (250 mL) and kept in the refrigerator (4℃) for later measuring the carbon concentration in rainfall (TC_{CP}), including dissolved organic carbon concentration (OC_{CP}) and dissolved inorganic carbon concentration (IC_{CP}) in the laboratory.

2.3. Laboratory analysis

Sample pretreatments were conducted at the State Key Laboratory of Urban and Regional Ecology, Research Center for Eco-Environmental Sciences, Chinese Academy of Sciences. After solid samples had been air-dried in the laboratory and sieved through a 2 mm screen.

A SHIMADZU-TOC-VCPH (with SSM-5000A solid element) instrument at the Key Laboratory of Tibetan Environment Changes and Land Surface Process, Institute of Tibetan Plateau Research, Chinese Academy of Sciences in Beijing was used for estimating the TC_{CS}, including OC_{CS} and IC_{CS}, in sediments. About 0.2 g soil in each sample was taken and sieved through a 0.075 mm screen. The analyses were performed on air-dried sediment samples. The output value of the instrument was TC and IC, the OC was equal to the difference of TC and IC.

The TC_{CP}, TC_{CR} and TC_{CI} were estimated using a Vario TOC analyzer (An instrument at the Research Center for Eco-Environmental Sciences, Chinese Academy of Sciences in Beijing). Filtered samples of 0.45 μm were analyzed immediately after sampling or, in the event of a backlog, refrigerated at 4℃ until analysis could proceed. Standard solutions of 0, 10, 50 and 100 ppm carbon were made, using 0, 1, 5 and 10 ml of stock solution, prepared by dissolving 2.125 g of the oven-dried reagent 'potassium hydrogen phthalate' ($C_8H_5KO_4$) in 1000 ml of distilled water. The output value of the instrument was TC and IC, the OC was equal to the difference of TC and IC.

2.4. Data analyses

Statistical analysis of data was performed using the software SPSS 21.0 for Windows. The mean values of the two replicate samples were used to estimate carbon concentration in infiltration water. ANOVA is used to describe the differences of rainfall between plots. T-tests at two-tailed are used to describe the differences between carbon fluxes by biophysical regulations. Statistical significances of results were evaluated at $\alpha = 0.05$.

The topsoil carbon flux by biophysical regulations (TC) induced by rainfall storms, including the carbon flux by rainfall (TC_P), runoff (TC_R), sediment (TC_S), and infiltration (TC_I), was equal to the sum of organic carbon (OC) fluxes and inorganic carbon (IC) fluxes:

$$TC = OC + IC \quad (1)$$

Total topsoil carbon flux by biophysical regulations (STC) during the study period was equal to the sum of those fluxes measured in all the rainfall events indicated by the subscripts:

$$STC = \sum TC_i,\ i = 1,2,3,\ldots, 9 \quad (2)$$

TC_P, TC_R, TC_S and TC_I, were calculated as the product of different carbon fluxes and carbon concentration of the corresponding carbon fluxes:

$$TC_P = TC_{CP} \times P \quad (3)$$

$$TC_R = TC_{CR} \times R \quad (4)$$

$$TC_S = TC_{CS} \times S \quad (5)$$

$$TC_I = TC_{CI} \times I \quad (6)$$

Net topsoil carbon flux by biophysical regulations (NTC) was calculated as the difference of TC_P minus carbon effluxes (TC_E) from topsoil (including TC_R,TC_S, and TC_I):

$$NTC = TC_P - (TC_R + TC_S + TC_I) \quad (7)$$

Total carbon efflux by biophysical regulations from topsoil (STC_E) and total net topsoil carbon flux by biophysical regulations (SNTC) were calculated as the sum of those fluxes

measured in all the rainfall events indicated by the subscripts:

$$STC_E = \sum TC_{Ei},\ i=1,2,3,\ldots,9 \quad (8)$$

$$SNTC = \sum NTC_i,\ i=1,2,3,\ldots,9 \quad (9)$$

The data that support the findings of this study are available from the corresponding author upon reasonable request.

3. Results

3.1. Erosion characteristics

There were no significant rainfall differences between the plots during the study period ($p=1>0.05$, $df=3$, $F=0.003$). Rainfall intensity ranged from 0.9 to 5.5 mm hr^{-1}. The total rainfall during the observation period was 254.1 mm. The heaviest rainfall (70.1±0.3 mm) occurred on 20th July while the lightest (6.6±0.4 mm) occurred on 7th September. The largest rainfall intensity occurred on 28th July.

The runoff, sediment yield, and infiltration characteristics in different plots changed greatly for different sampling dates (Figure S1). Most runoff occurred on 13th September but most sediment was observed on 17th August. When the rainfall intensity was less than 1.3 mm hr^{-1}, there was no runoff and sediment occurred. The most infiltration happened on 20th July and the least happened on 7th September.

The sediment yield and runoff in the plots with vegetation were much less than in the plot without vegetation, but the infiltration was more in the plots with vegetation than in the plot without vegetation. Data suggests that vegetation cover reduces runoff and sediment yield significantly (Figure S1). The function of reducing runoff and sediment yield compared to the plot without vegetation was weakest in the S2 plot. The seven plots with vegetation all showed that vegetation plays a very important role in decreasing sediment yield - by more than 98% on average.

3.2. Topsoil carbon fluxes by biophysical regulations

Total topsoil carbon input by rainfall (STC_P) was relatively small, with total organic carbon input flux by rainfall (SOC_P) the predominant form. The SOC_Ps were positively related to rainfall/throughfall ($p<0.01$) (see Figure 2). Some linear relationships (in Figure 2) were evident between SOC_Ps and rainfall/throughfall amount. The relationships between total inorganic carbon flux by rainfall (SIC_P) and rainfall/throughfall amount were not significant ($p>0.05$) (Figure 2).

The total organic carbon flux by runoff (SOC_R) (0.61 ± 0.31 g m^{-2}) was much higher than the inorganic carbon flux by runoff (SIC_R) (0.05 ± 0.04 g m^{-2}) (Figure 3). Total carbon flux by runoff (STC_R) from plot with vegetation (0.55 ± 0.19 g m^{-2}) was reduced compared to plot without vegetation (1.39 g m^{-2}). There were no significant differences ($p=0.534>0.05$, $t=0.641$, $df=12$) between total organic carbon flux by sediment (SOC_S) (0.21 ± 0.08 g m^{-2}) and inorganic carbon flux by sediment (SIC_S) (0.25 ± 0.10 g m^{-2}) in plots with vegetation (Figure 3). The total carbon flux by sediment (STC_S) from the CK plot (30.11 g m^{-2}) is much more

than the other plots with vegetation (0.46±0.18 g m^{-2}). The total organic carbon flux by infiltration (SOC_I) (22.13±2.76 g m^{-2}) was much more than inorganic carbon flux by infiltration (SIC_I) (4.59±0.86 g m^{-2}) in Figure 3. The differences between plots with vegetation and without vegetation were based on vegetation types. The total carbon flux by infiltration (STC_I) from the plot with woody vegetation (25.17±4.23 g m^{-2}) was less than that from plot without vegetation (28.45 g m^{-2}). However, the STC_I from the plot with non-woody vegetation (28.23±0.71 g m^{-2}) was nearly the same as that from plot without vegetation (28.45 g m^{-2}).

In Figure 3, the STC_E was mainly in the form of total organic carbon efflux (SOC_E) for the higher OC concentration compared to IC concentration in DC effluxes (Table S2). The STC_E from the CK plot (SOC_E was 38.56 g m^{-2}, total inorganic carbon efflux (SIC_E) was 21.39 g m^{-2}) was much greater than that from the plots with vegetation (41.3±7.8% more for SOC_E and 77.4±4.2% more for SIC_E). The SOC_E was 4.8 (±0.7) times more than SIC_E in plots with vegetation.

The SOC_I in plots with woody vegetation (A1, A2, S1, and S2) (20.57±3.34 g m^{-2}) was less than in plots with non-woody vegetation (H1, H2, and H3) (23.74±0.39 g m^{-2}). Compared to woody vegetation cover, the non-woody vegetation increased the SOC_I. The SOC_E in plots with woody vegetation (21.31±3.50 g m^{-2}) was less than in plots with non-woody vegetation (24.44±0.58 g m^{-2}) (Figure 3). The differences of SIC_E between plots with woody vegetation (4.90±1.21 g m^{-2}) and non-woody vegetation (4.73±0.41 g m^{-2}) were not significant ($p=0.606>0.05$, $t=0.550$, $df=5$). It meant that the woody vegetation cover

played a more important role in reducing SOC_E than non-woody vegetation.

3.3. Partitioning of total topsoil carbon efflux by biophysical regulations

STC_I made up most (96.8±0.9% in SOC_E, 93.9±2.9% in SIC_E) of STC_E in plots with vegetation (Figure 3). Compared to the ratio (61.0% in SOC_E, 22.9% in SIC_E) in the CK plot, we found that vegetation considerably increased the contribution of STC_I. Compared to the part of the STC_S from the CK plot (35.7% in SOC_E, 76.4% in SIC_E), the vegetation greatly reduced the contribution of STC_S (0.9±0.4% in SOC_E and 5.2±2.6% in SIC_E for plots with vegetation). For the IC_{CS} was more than OC_{CS} (Table S2), the percent of SIC_S was much more than that of SOC_S. However, the contribution of STC_R changed little between plots with vegetation (2.3±0.7% in SOC_E, 0.8±0.4% in SIC_E) and without vegetation (3.2% in SOC_E, 0.7% in SIC_E).

3.4. Contribution of carbon fluxes by biophysical regulations to carbon sequestration rate

Our results showed that water-driven erosion and infiltration resulted in a net loss of carbon from topsoil. SNTC was -25.4 ±3.3 g m^{-2} in plot with vegetation and -57.8 g m^{-2} in plot without vegetation. The ratio of total net topsoil carbon flux by biophysical regulations compared to soil carbon sequestration rate (SNTC:CSR) is a good indicator to explain the importance of carbon flux by biophysical regulations. Using the typical CSR of about 29 gC m^{-2} yr^{-1} in the region (Chang et al., 2011; Deng et al., 2014a), the SNTC:CSR ratio was estimated to be 0.71 ±0.10 on average for the seven plots with vegetation. The ratio of

SNTC:CSR was smallest (0.54) in S1 plot and highest (0.79) in H2 plot among the seven plots. Although the TC_I is a net loss of carbon from the topsoil layer, this might not be reflected at the terrestrial ecosystem level as it enters deeper layers. The STC_I was estimated to be 76 ±10 % of the CSR in this region.

4. Discussion

4.1. Carbon flux by infiltration is important in ecological restoration area

Two main factors determine the TC_I: infiltration flux (I) and carbon concentration (TC_{CI}). In the CK and non-woody vegetation plots, there was effectively no rainfall interception. Although the infiltration increased for the non-woody vegetation cover, the differences of infiltration between CK plot and non-woody vegetation plot (Figure S1) was minimal. The infiltration in plots with woody vegetation was less than that in the CK plot. The TC_{CI} differences between plots with and without vegetation were not significant ($p>0.05$).

The differences between plots with and without vegetation showed that vegetation cover increases the contribution of STC_I in STC_E (Figure 3). The main reason for the increment of contribution of STC_I was the reduction of STC_S. STC_S was reduced much in plots with vegetation compared to plots without vegetation (Figure 3). The decrement was associated closely with the sediment yield during water-driven erosion. Sediment yield was reduced for the vegetation restoration (Fu et al., 2017; Li et al., 2015; Puigdefábregas, 2005). The STC_S also decreased; an expected result given the positive relationship between TC_S and sediment yield (Boix-Fayos et al., 2015; Li et al., 2016; Müller-Nedebock & Chaplot, 2015; Nie et al.,

2014).

TC_I was the most important TC_E in the restored areas (Figure 3). This is in contrast with previous studies (Lowrance & Williams, 1988; Nie et al., 2014) that suggested sediment-bound carbon flux was mainly topsoil carbon efflux resulting from biophysical regulations. The differences we observed were likely caused by the experimental setting. Lowrance et al. (1988) did not observe the same degree of TC_I. In fact, there a few studies elaborate DC fluxes by soil erosion (Doetterl et al., 2016). DC effluxes from topsoil (including TC_R and TC_I) will be more and more important in ecological restoration area. For example, since the end of 1970s, the ‘‘Grain for Green Project’’ on the Loess Plateau has played an important role in reducing soil erosion by increasing vegetation cover (Fu et al., 2017; Zhang et al., 2014). Under the ‘‘Grain for Green Project’’, vegetation coverage on the Loess Plateau increased from 50% to nearly 60% (Fu et al., 2017). An average decrease of 10.3 mm yr^{-1} across the whole Loess Plateau between 2002 and 2008 was observed by Feng et al.(2012). The average annual sediment yield also decreased from 7,576 t km^{-2} yr^{-1} (during 1955–1969) to 975 t km^{-2} yr^{-1} (during 2000–2009); a reduction of 87% (Xin et al., 2012). TC_R and TC_S were reduced with runoff and sediment yield in consequence. The division of TC_E seems to have changed as a result of vegetation restoration. DC efflux has been the largest carbon efflux by biophysical regulations on the Loess Plateau.

4.2. A potential underestimated carbon sequestration capacity in restored areas

STC_I contributed to about 96% of STC_E (Figure 3). This result fits well with previous studies that observed TC_I (Rumpel & Kogel-Knabner, 2011). In reality, TC_I is not easily

observable (Doetterl et al., 2016; Lal, 2003; Yue et al., 2016). In addition, CSR are typically estimated by measuring changes in the carbon storage of topsoil layers (Deng et al., 2017; Wang et al., 2011). Most previous estimates of CSR at the ecosystem level might have been underestimated because these measurements have been estimated using measurements of carbon storage change in the topsoil layer without considering carbon flux by biophysical regulations in other soil layers, particularly carbon percolation (Figure 4A).

The fate of percolated carbon is not certain. The percolated carbon may be drained out by base flow or decompose by mineralization. It can also be stay in the deeper soil layers according to previous studies (Ma et al., 2014; Rumpel & Kogel-Knabner, 2011). If percolated carbon is not included in SC estimation methods, total ecosystem carbon sequestration may be underestimated. The actual carbon sequestration rate (CSRa) should be equal to the sum of known CSR and TC_I, if the dynamic replacement hypothesis of carbon in the topsoil layer (Stallard, 1998; Harden et al., 1999) holds and the percolated carbon is protected from decomposition in the deep layers (Figure 4B). The estimated CSRa (48.0 gC m^{-2} yr^{-1} in A1 plot, 52.3 gC m^{-2} yr^{-1} in A2 plot, 45.6 gC m^{-2} yr^{-1} in S1 plot, 52.3 gC m^{-2} yr^{-1} in S2 plot, 52.4 gC m^{-2} yr^{-1} in H1 plot, 53.2 gC m^{-2} yr^{-1} in H2 plot, and 52.7 gC m^{-2} yr^{-1} in H3 plot) was 50.9 ±2.9 gC m^{-2} yr^{-1}. This means that the previous CSR might have been underestimated by as large as 43±3%. Carbon flux by biophysical regulations is likely to play an important role in affecting the carbon dynamics in topsoil layers as well as in deep layers.

4.3. The expansion of the dynamic carbon replacement hypothesis

Although the SNTCs were a net carbon source in the topsoil layers, the lost carbon from

topsoil layers will be replaced by sequestering new carbon from the atmosphere (mainly by production of new photosynthate) at the eroding sites (i.e., the so-called dynamic carbon replacement hypothesis) (Harden et al., 1999; Liu et al., 2003; Stallard, 1998)(Figure 4A). This concept of the 'dynamic carbon replacement hypothesis' focused only on the lateral carbon flux by soil erosion (Harden et al., 2008; Stallard, 1998; Van Oost et al., 2008). Based on the results of our study, we argue that the dynamic carbon replacement hypothesis should be broadened to include vertical carbon flux by infiltration (Figure 4B). In addition, the vertical carbon flux (i.e., infiltration) might be much larger than the lateral carbon fluxes. The carbon lost by infiltration will also be replaced by photosynthesis and vegetation roots in the deep soil layers. Therefore, including the vertical carbon flux from the topsoil layer or other soil layers into the dynamic carbon replacement scheme is a crucial step forward.

4.4. The fate of infiltrated carbon

Vertical carbon efflux from topsoil is an important carbon translocation process. The lost carbon from topsoil layers to deeper soil layers cannot be neglected. However, understanding the fate of the infiltrated or percolated carbon in the deep layers is still a major challenge. It is likely some of the infiltrated carbon will be decomposed as it moves down the soil profile while some will be retained and protected from decomposition (Deng et al., 2014a; Neff & Asner, 2001).

The fate of infiltrated carbon can be complex. Many authors observed a sharp decrease of dissolved organic carbon (DOC) concentrations with depth of mineral soil (Kaiser & Zech, 1997; Qualls & Haines, 1992). Several studies (Rumpel et al., 2010; Rumpel et al., 2004)

suggest that soil organic carbon in subsoil is enriched in microbial-derived carbon compounds and depleted in energy-rich plant material compared to that in topsoil. Therefore, whether the infiltrated carbon retention in subsoil is stable or prone to decomposition is still unknown (Ma et al., 2014; Rumpel & Kogel-Knabner, 2011).

5. Conclusions

In summary, we observed the topsoil carbon flux by biophysical regulations in the field during rainfall storms in a growing season. The objective was to develop a better understanding of the role of water-driven erosion and infiltration in causing carbon flux by biophysical regulations and to investigate the quantitative relationships among different carbon fluxes and influencing factors. First, TC_I was the most important carbon efflux by biophysical regulations from topsoil in plots with vegetation. STC_I is largest (about 96%) in STC_E. In plot without vegetation, STC_S occupies about 50% in STC_E, which is the largest carbon efflux from topsoil. Second, just considering topsoil carbon flux by biophysical regulations, carbon sequestration capacity may be underestimated by up to 43 ±3 %. The TC_I is a loss from the topsoil layer, but a gain at the terrestrial ecosystem level as it might not be lost as it enters deep layers. If not accounted for, the total ecosystem carbon sequestration might be underestimated. Third, topsoil carbon fluxes by biophysical regulations played an important role in affecting SC pools dynamics. SNTC is net carbon source to the deep layer and the magnitude was about 71 ±10% of the typical CSR in the region. Our research calls for broadening the dynamic carbon replacement hypothesis to include vertical carbon lost by infiltration from the top soil layer. This expansion of the theoretical framework is

fundamental as it includes all carbon major fluxes by biophysical regulations, and the newly added vertical fluxes might be more important than the lateral fluxes.

Acknowledgements

This work was funded by National Key Research and Development Program of China (No. 2017YFA0604701), National Natural Science Foundation of China (No. 41390464) and the Chinese Academy of Sciences (No. QYZDY-SSW-DQC025). We thank Weiliang Chen, Jian Wang, Mengmeng Zhang and Weiwei Fang for observational data and suggestions that led to clarification of various aspects in the manuscript. We thank Prof. John Gash for his assistance with the English language editing.

Competing interests

The authors declare no competing financial interests.

Supplementary information

The supplementary figures and tables are listed after the main body, which start with Table S and Figure S.

References

Aitkenhead-Peterson JA, Smart RP, Aitkenhead MJ, Cresser MS, McDowell WH. 2007. Spatial and temporal variation of dissolved organic carbon export from gauged and ungauged watersheds of Dee Valley, Scotland: Effect of land cover and C:N. *Water Resources Research* **43**: 160-161. DOI: 10.1029/2006wr004999

Alvarez-Cobelas M, Angeler DG, Sánchez-Carrillo S, Almendros G. 2012. A worldwide view

of organic carbon export from catchments. *Biogeochemistry* **107**: 275-293. DOI: 10.1007/s10533-010-9553-z

Boix-Fayos C, Nadeu E, Quiñonero JM, Martínez-Mena M, Almagro M, de Vente J. 2015. Sediment flow paths and associated organic carbon dynamics across a Mediterranean catchment. *Hydrology and Earth System Sciences* **19**: 1209-1223. DOI: 10.5194/hess-19-1209-2015

Bouchoms S, Wang Z, Vanacker V, Doetterl S, Van Oost K. 2017. Modelling long-term soil organic carbon dynamics under the impact of land cover change and soil redistribution. *Catena* **151**: 63-73. DOI: 10.1016/j.catena.2016.12.008

Bremenfeld S, Fiener P, Govers G. 2013. Effects of interrill erosion, soil crusting and soil aggregate breakdown on in situ CO_2 effluxes. *Catena* **104**: 14-20. DOI: 10.1016/j.catena.2012.12.011

Brye KR, Norman JM, Bundy LG, Gower ST. 2001. Nitrogen and carbon leaching in agroecosystems and their role in denitrification potential. *Journal of Environmental Quality* **30**: 58. DOI: 10.2134/jeq2001.30158x

Chang R, Fu B, Liu G, Liu S. 2011. Soil carbon sequestration potential for "Grain for Green" project in Loess Plateau, China. *Environmental Management* **48**: 1158-72. DOI: 10.1007/s00267-011-9682-8

Chappell A, Baldock J, Sanderman J. 2015. The global significance of omitting soil erosion from soil organic carbon cycling schemes. *Nature Climate Change* **6**: 187-191. DOI:

10.1038/nclimate2829

Clark MJ, Cresser MS, Smart R, Chapman PJ, Edwards AC. 2004. The influence of catchment characteristics on the seasonality of carbon and nitrogen species concentrations in upland rivers of Northern Scotland. *Biogeochemistry* **68**: 1-19. DOI: 10.1023/B:BIOG.0000025733.07568.11

Deng L, Liu GB, Shangguan ZP. 2014a. Land-use conversion and changing soil carbon stocks in China's 'Grain-for-Green' Program: a synthesis. *Global Change Biology* **20**: 3544-56. DOI: 10.1111/gcb.12508

Deng L, Liu S, Kim DG, Peng C, Sweeney S, Shangguan Z. 2017. Past and future carbon sequestration benefits of China's grain for green program. *Global Environmental Change* **47**: 13-20. DOI: 10.1016/j.gloenvcha.2017.09.006

Deng L, Shangguan ZP, Sweeney S. 2014b. "Grain for Green" driven land use change and carbon sequestration on the Loess Plateau, China. *Scientific Reports* **4**: 7039. DOI: 10.1038/srep07039

Doetterl S, Berhe AA, Nadeu E, Wang Z, Sommer M, Fiener P. 2016. Erosion, deposition and soil carbon: A review of process-level controls, experimental tools and models to address C cycling in dynamic landscapes. *Earth-Science Reviews* **154**: 102-122. DOI: 10.1016/j.earscirev.2015.12.005

Elena C, Tiziana D, Michele I, Elio C, Marta AR, Antonietta F, Stefania P. 2017. Soil characterization and comparison of organic matter quality and quantity of two stands under

different vegetation cover on Monte Faito (Campania, S-Italy). In *18th International Symposium on Environmental Pollution and its Impact on Life in the Mediterranean Region (MESAEP)*. FRESENIUS ENVIRONMENTAL BULLETIN: Crete, GREECE; 8-18.

Feng XM, Sun G, Fu BJ, Su CH, Liu Y, Lamparski H. 2012. Regional effects of vegetation restoration on water yield across the Loess Plateau, China. *Hydrology & Earth Systemences* **16**: 4161-4191. DOI: 10.5194/hess-16-2617-2012

Fu B, Wang S, Liu Y, Liu J, Liang W, Miao C. 2017. Hydrogeomorphic ecosystem responses to natural and anthropogenic changes in the Loess Plateau of China. *Annual Review of Earth and Planetary Sciences* **45**: 223-243. DOI: 10.1146/annurev-earth-063016-020552

Gauder M, Billen N, Zikeli S, Laub M, Graeff-Hönninger S, Claupein W. 2016. Soil carbon stocks in different bioenergy cropping systems including subsoil. *Soil and Tillage Research* **155**: 308-317. DOI: 10.1016/j.still.2015.09.005

Harden J, Sharpe J, Parton W, Ojima D, Fries T, Huntington T, Dabney S. 1999. Dynamic replacement and loss of soil carbon on eroding cropland. *Global Biogeochemical Cycles* **13**: 885-901. DOI: 10.1029/1999GB900061

Harden JW, Berhe AA, Torn M, Harte J, Liu S, Stallard RF. 2008. Soil erosion: Data say C sink. *Science* **320**: 178-179. DOI: 10.1126/science.320.5873.178

Hemelryck HV, Fiener P, Oost KV, Govers G, Merckx R. 2010. The effect of soil redistribution on soil organic carbon: an experimental study. *Biogeosciences* **7**: 3971-3986. DOI: 10.5194/bg-7-3971-2010

Hu PL, Liu SJ, Ye YY, Zhang W, Wang KL, Su YR. 2018. Effects of environmental factors on soil organic carbon under natural or managed vegetation restoration. *Land Degradation & Development* **29**: 387-397. DOI: 10.1002/ldr.2876

Jacinthe PA, Lal R, Owens LB, Hothem DL. 2004. Transport of labile carbon in runoff as affected by land use and rainfall characteristics. *Soil and Tillage Research* **77**: 111-123. DOI: 10.1016/j.still.2003.11.004

Jiao L, Lu N, Sun G, Ward EJ, Fu B. 2016. Biophysical controls on canopy transpiration in a black locust (Robinia pseudoacacia) plantation on the semi-arid Loess Plateau, China. *Ecohydrology* **9**: 1068-1081. DOI: 10.1002/eco.1711

Kaiser K, Zech W. 1997. Competitive sorption of dissolved organic matter fractions to soils and related mineral phases. *Soil Science Society of America Journal* **61**: 64-69. DOI: 10.2136/sssaj1997.03615995006100010011x

Kindler R, Siemens JAN, Kaiser K, Walmsley DC, Bernhofer C, Buchmann N, Cellier P, Eugster W, Gleixner G, GrÜNwald T, Heim A, Ibrom A, Jones SK, Jones M, Klumpp K, Kutsch W, Larsen KS, Lehuger S, Loubet B, McKenzie R, Moors E, Osborne B, Pilegaard KIM, Rebmann C, Saunders M, Schmidt MWI, Schrumpf M, Seyfferth J, Skiba UTE, Soussana J-F, Sutton MA, Tefs C, Vowinckel B, Zeeman MJ, Kaupenjohann M. 2011. Dissolved carbon leaching from soil is a crucial component of the net ecosystem carbon balance. *Global Change Biology* **17**: 1167-1185. DOI: 10.1111/j.1365-2486.2010.02282.x

Lal R. 2003. Soil erosion and the global carbon budget. *Environment International* **29**:

437-450. DOI: 10.1016/s0160-4120(02)00192-7

Lal R. 2004. Soil carbon sequestration impacts on global climate change and food security. *Science* **304**: 1623-1627. DOI: 10.1126/science.1097396

Lal R, Pimentel D. 2008. Soil erosion: A carbon sink or source? *Science* **319**: 1040-1042. DOI: 10.1126/science.319.5866.1040

Li J, Zhang F, Wang S, Yang M. 2015. Combined influences of wheat-seedling cover and antecedent soil moisture on sheet erosion in small-flumes. *Soil and Tillage Research* **151**: 1-8. DOI: 10.1016/j.still.2015.02.006

Li Y, Poesen J, Yang JC, Fu B, Zhang JH. 2003. Evaluating gully erosion using 137Cs and 210Pb/137Cs ratio in a reservoir catchment. *Soil and Tillage Research* **69**: 107-115. DOI: 10.1016/S0167-1987(02)00132-0

Li Z, Nie X, Chang X, Liu L, Sun L. 2016. Characteristics of soil and organic carbon loss induced by water erosion on the Loess Plateau in China. *PLoS One* **11**: e0154591. DOI: 10.1371/journal.pone.0154591

Liu S, Bliss N, Sundquist E, Huntington TG. 2003. Modeling carbon dynamics in vegetation and soil under the impact of soil erosion and deposition. *Global Biogeochemical Cycles* **17**: 187-194. DOI: 10.1029/2002GB002010

Lowrance R, Williams RG. 1988. Carbon movement in runoff and erosion under simulated rainfall conditions. *Soil Science Society of America Journal* **52**: 1445–1448. DOI: 10.2136/sssaj1988.03615995005200050045x

Müller-Nedebock D, Chaplot V. 2015. Soil carbon losses by sheet erosion: a potentially critical contribution to the global carbon cycle. *Earth Surface Processes and Landforms* **40**: 1803-1813. DOI: 10.1002/esp.3758

Ma W, Li Z, Ding K, Huang J, Nie X, Zeng G, Wang S, Liu G. 2014. Effect of soil erosion on dissolved organic carbon redistribution in subtropical red soil under rainfall simulation. *Geomorphology* **226**: 217-225. DOI: 10.1016/j.geomorph.2014.08.017

Martinez-Mena M, Lopez J, Almagro M, Boix-Fayos C, Albaladejo J. 2008. Effect of water erosion and cultivation on the soil carbon stock in a semiarid area of South-East Spain. *Soil and Tillage Research* **99**: 119-129. DOI: 10.1016/j.still.2008.01.009

Neff JC, Asner GP. 2001. Dissolved organic carbon in terrestrial ecosystems: synthesis and a model. *Ecosystems* **4**: 29-48. DOI: 10.1007/s100210000058

Nie X, Li Z, Huang J, Huang B, Zhang Y, Ma W, Hu Y, Zeng G. 2014. Soil organic carbon loss and selective transportation under field simulated rainfall events. *PLoS One* **9**: e105927. DOI: 10.1371/journal.pone.0105927

Nie XJ, Zhang JH, Cheng JX, Gao H, Guan ZM. 2016. Effect of soil redistribution on various organic carbons in a water- and tillage-eroded soil. *Soil and Tillage Research* **155**: 1-8. DOI: 10.1016/j.still.2015.07.003

Pohl M, Graf F, Buttler A, Rixen C. 2012. The relationship between plant species richness and soil aggregate stability can depend on disturbance. *Plant and Soil* **355**: 87-102. DOI: 10.1007/s11104-011-1083-5

Polyakov VO, Lal R. 2004. Soil erosion and carbon dynamics under simulated rainfall. *Soil Science* **169**: 590-599. DOI: 10.1097/01.ss.0000138414.84427.40

Puigdefábregas J. 2005. The role of vegetation patterns in structuring runoff and sediment fluxes in drylands. *Earth Surface Processes and Landforms* **30**: 133-147. DOI: 10.1002/esp.1181

Qualls RG, Haines BL. 1992. Biodegradability of dissloved organic-matter in forest throughfall, soil solution, and stream water. *Soil Science Society of America Journal* **56**: 578-586. DOI: 10.2136/sssaj1992.03615995005600020038x

Quinton JN, Catt JA, Wood GA, Steer J. 2006. Soil carbon losses by water erosion: Experimentation and modeling at field and national scales in the UK. *Agriculture Ecosystems & Environment* **112**: 87-102. DOI: 10.1016/j.agee.2005.07.005

Razafimbelo TM, Albrecht A, Oliver R, Chevallier T, Chapuis-Lardy L, Feller C. 2008. Aggregate associated-C and physical protection in a tropical clayey soil under Malagasy conventional and no-tillage systems. *Soil and Tillage Research* **98**: 140-149. DOI: 10.1016/j.still.2007.10.012

Rieckh H, Gerke HH, Siemens J, Sommer M. 2014. Water and Dissolved Carbon Fluxes in an Eroding Soil Landscape Depending on Terrain Position. *Vadose Zone Journal* **13**: 1-14. DOI: 10.2136/vzj2013.10.0173

Rumpel C, Eusterhues K, Kögel-Knabner I. 2010. Non-cellulosic neutral sugar contribution to mineral associated organic matter in top- and subsoil horizons of two acid forest soils. *Soil*

Biology & Biochemistry **42**: 379-382. DOI: 10.1016/j.soilbio.2009.11.004

Rumpel C, Eusterhues K, Kogelknabner I. 2004. Location and chemical composition of stabilized organic carbon in topsoil and subsoil horizons of two acid forest soils. *Soil Biology & Biochemistry* **36**: 177-190. DOI: 10.1016/j.soilbio.2003.09.005

Rumpel C, Kogel-Knabner I. 2011. Deep soil organic matter-a key but poorly understood component of terrestrial C cycle. *Plant and Soil* **338**: 143-158. DOI: 10.1007/s11104-010-0391-5

Schiettecatte W, Gabriels D, Cornelis WM, Hofman G. 2008a. Enrichment of organic carbon in sediment transport by interrill and rill erosion processes. *Soil Science Society of America Journal* **72**: 50. DOI: 10.2136/sssaj2007.0201

Schiettecatte W, Gabriels D, Cornelis WM, Hofman G. 2008b. Impact of deposition on the enrichment of organic carbon in eroded sediment. *Catena* **72**: 340-347. DOI: 10.1016/j.catena.2007.07.001

Schreiber JD. 1999. Nutrient leaching from corn residues under simulated rainfall. *Journal of Environmental Quality* **28**: 1864-1870. DOI: 10.2134/jeq1999.00472425002800060024x

Stallard RF. 1998. Terrestrial sedimentation and the carbon cycle: Coupling weathering and erosion to carbon burial. *Global Biogeochemical Cycles* **12**: 231-257. DOI: 10.1029/98gb00741

Van Oost K, Six J, Govers G, Quine T, De Gryze S. 2008. Soil erosion: A carbon sink or source? Response. *Science* **319**: 1042-1042

Wang X, Cammeraat ELH, Romeijn P, Kalbitz K. 2014. Soil organic carbon redistribution by water erosion – The role of CO_2 emissions for the carbon budget. *PLoS One* **9**: e96299. DOI: 10.1371/journal.pone.0096299

Wang Y, Fu B, Lue Y, Chen L. 2011. Effects of vegetation restoration on soil organic carbon sequestration at multiple scales in semi-arid Loess Plateau, China. *Catena* **85**: 58-66. DOI: 10.1016/j.catena.2010.12.003

Wang Z, Hoffmann T, Six J, Kaplan JO, Govers G, Doetterl S, Van Oost K. 2017. Human-induced erosion has offset one-third of carbon emissions from land cover change. *Nature Climate Change* **7**: 345. DOI: 10.1038/nclimate3263

Xin Z, Ran L, Lu XX. 2012. Soil Erosion Control and Sediment Load Reduction in the Loess Plateau: Policy Perspectives. *International Journal of Water Resources Development* **28**: 325-341. DOI: 10.1080/07900627.2012.668650

Young CJ, Liu SG, Schumacher JA, Schumacher TE, Kaspar TC, McCarty GW, Napton D, Jaynes DB. 2014. Evaluation of a model framework to estimate soil and soil organic carbon redistribution by water and tillage using Cs-137 in two US Midwest agricultural fields. *Geoderma* **232**: 437-448. DOI: 10.1016/j.geoderma.2014.05.019

Yue Y, Ni J, Ciais P, Piao S, Wang T, Huang M, Borthwick AGL, Li T, Wang Y, Chappell A, Van Oost K. 2016. Lateral transport of soil carbon and land−atmosphere CO_2 flux induced by water erosion in China. *Proceedings of the National Academy of Sciences of the United States of America* **113**: 6617-6622. DOI: 10.1073/pnas.1523358113

Zhang H, Liu S, Yuan W, Dong W, Ye A, Xie X, Chen Y, Liu D, Cai W, Mao Y. 2014. Inclusion of soil carbon lateral movement alters terrestrial carbon budget in China. *Scientific Reports* **4**: 7247. DOI: 10.1038/srep07247

Zhang JH, Wang Y, Li FC. 2015. Soil organic carbon and nitrogen losses due to soil erosion and cropping in a sloping terrace landscape. *Soil Research* **53**: 87-96. DOI: 10.1071/sr14151

Zhang X, Li ZW, Tang ZH, Zeng GM, Huang JQ, Guo W, Chen XL, Hirsh A. 2013. Effects of water erosion on the redistribution of soil organic carbon in the hilly red soil region of southern China. *Geomorphology* **197**: 137-144. DOI: 10.1016/j.geomorph.2013.05.004

Zhao P, Tang X, Zhao P, Wang C, Tang J. 2013. Identifying the water source for subsurface flow with deuterium and oxygen-18 isotopes of soil water collected from tension lysimeters and cores. *Journal of Hydrology* **503**: 1-10. DOI: 10.1016/j.jhydrol.2013.08.033

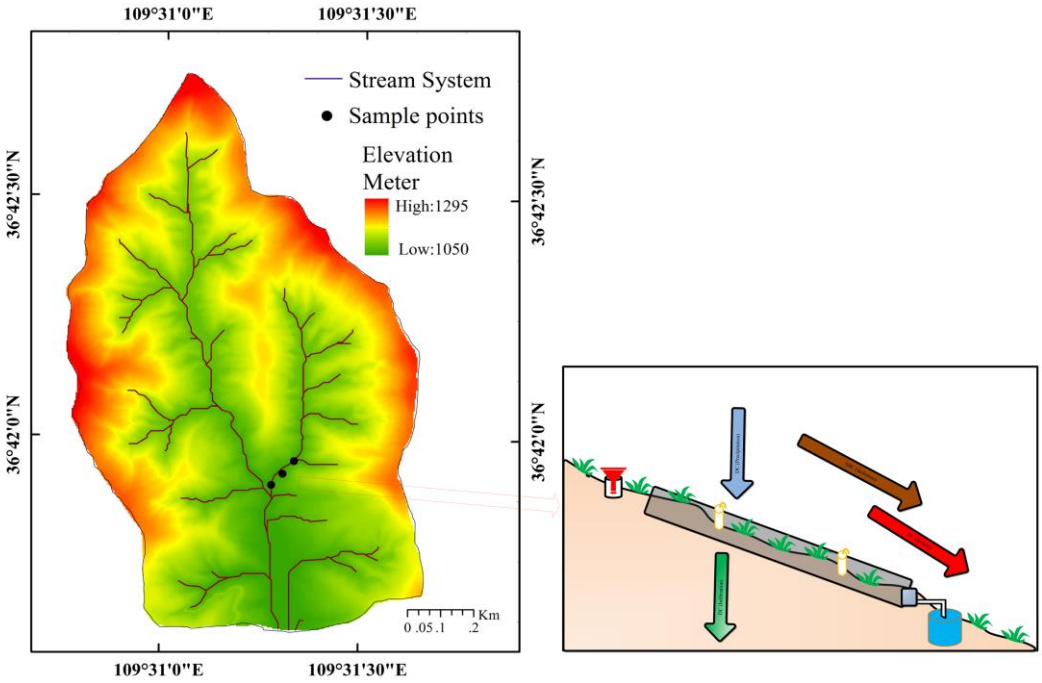

Figure 1. Location of the study region in China and the study plots. The inset shows the location of the study region in China. Schematic diagram of lateral and vertical carbon flux by biophysical regulations components during rainfall storms and the setup of experimental facility are in the bottom right corner. Different color represents different carbon flux by biophysical regulations. DC is dissolved carbon flux and SBC is the sediment-bound carbon flux. This map was created in ArcGIS 10.1.

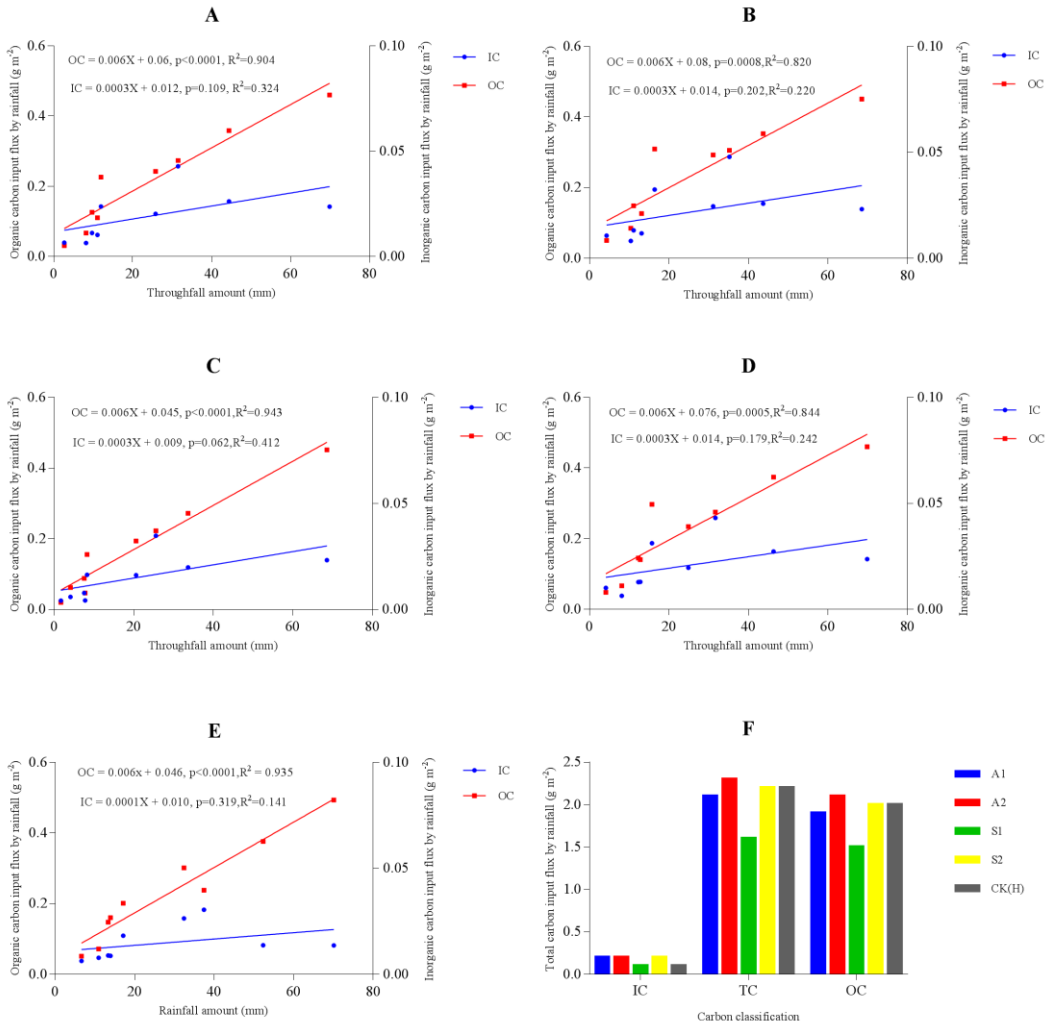

Figure 2. Topsoil carbon input flux by rainfall. The relationships between carbon input flux by rainfall and rainfall/throughfall amount for organic (OC) and inorganic carbon (IC) input flux are showed from A to E. The left Y axis is the organic carbon input flux and right Y axis is the inorganic carbon input flux. A, B, C, and D is in A1, A2, S1, and S2 plot, respectively. E represents the plot of H1, H2, H3 and CK with no rainfall interception. Each point represents a sampling date. F is the total biophysical carbon input flux by rainfall. Different color represents the carbon input flux in different plot. OC represents organic carbon, IC represents inorganic carbon and TC represents the sum of OC and IC.

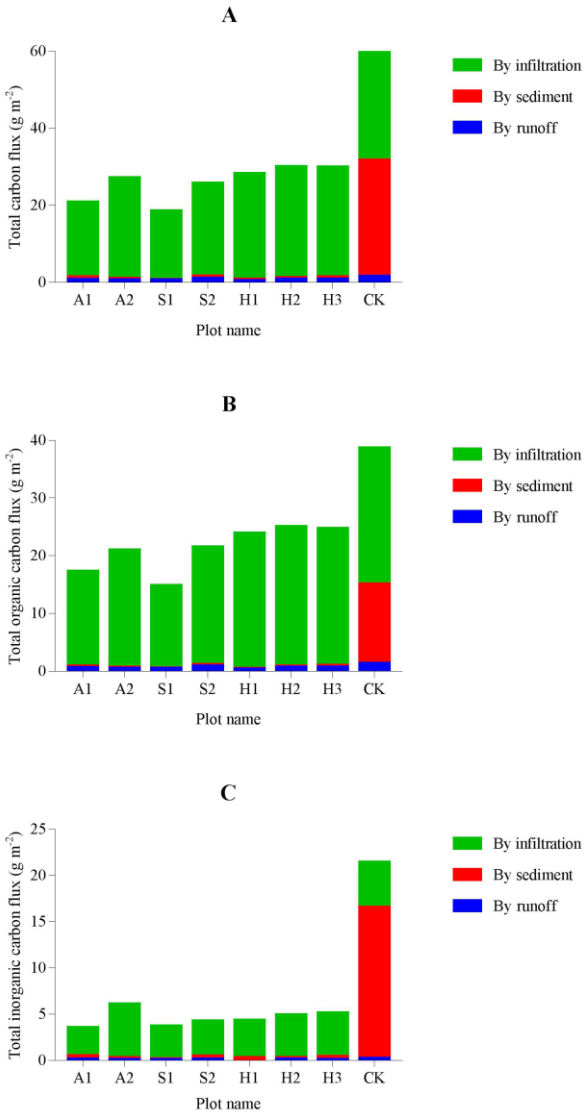

Figure 3. Partitioning of total topsoil carbon efflux by biophysical regulations. Total carbon flux (A), total organic carbon flux (B), and total inorganic carbon flux(C). The different color represents the topsoil carbon efflux by runoff, sediment and infiltration. The X axis is the different plots.

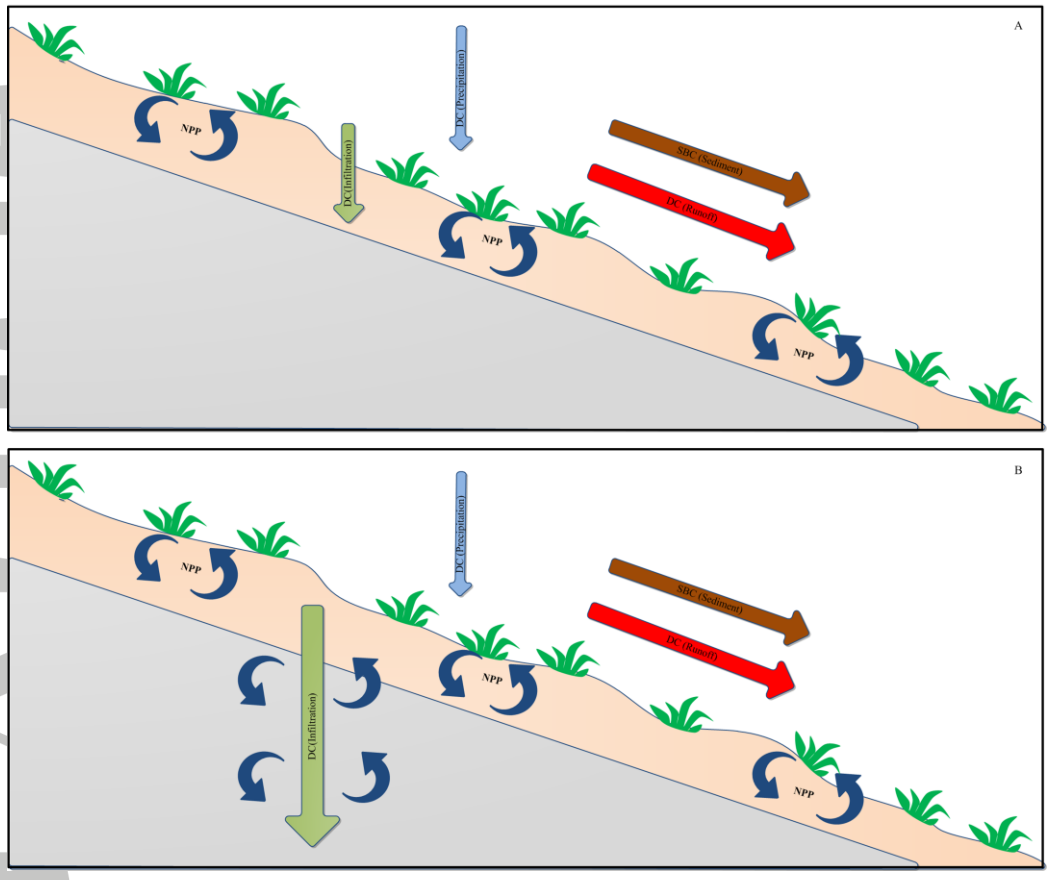

Figure 4. Schematic diagram of two kinds of dynamic carbon replacement hypothesis during water-driven erosion in an eroding landscape. A is the dynamic carbon replacement hypothesis including lateral soil carbon lost by erosion only. The eroded carbon is replaced mainly by production of new photosynthate. B is the expansion of the dynamic carbon replacement hypothesis including lateral carbon lost by erosion and vertical carbon lost by infiltration from topsoil layer. Photosynthesis replaces not only lateral carbon lost by erosion but also vertical carbon lost by infiltration. Different colors of arrows represent different topsoil carbon flux by biophysical regulations. SBC is the carbon flux by sediment. DC is the carbon flux by rainfall, runoff and infiltration.

Figure S1. Runoff, sediment yield, and infiltration characteristics on different sampling dates for: (A) runoff characteristics, (B) sediment yield characteristics, and (C) infiltration characteristics.